Role of vapor transfer on flow coating of colloidal dispersions in the evaporative regime

Charles Loussert[1], Frédéric Doumenc[2,3], Jean-Baptiste Salmon[1],
Vadim S. Nikolayev[4] and Béatrice Guerrier[2]

[1] CNRS, Solvay, LOF, UMR 5258, Univ. Bordeaux, F-33600 Pessac, France

[2] Laboratoire FAST, Univ. Paris-Sud, CNRS, Université Paris-Saclay, F-91405, Orsay, France

[3] Sorbonne Universités, UPMC Univ. Paris 06, UFR 919, 75005, Paris, France

[4] Service de Physique de l'État Condensé, CNRS , Université Paris-Saclay, CEA Saclay, 91191 Gif-Sur-Yvette, France

Corresponding author: charles.loussert-ex@solvay.com

Key words: coating, evaporative regime, film deposition, vapor transfer, colloids

Flow coating techniques, such as knife coating, blade coating, or doctor blade, have now become essential processes to coat continuously functional layers on solid substrates starting from dilute inks, and for applications ranging from organic electronics to optical coatings [1-3]. Figure 1 shows schematically a typical blade-coating setup for the specific case of a colloidal dispersion. A liquid film is drawn out of a liquid reservoir confined between a fixed blade and a moving substrate at a velocity V. The fine description of such flow-coating processes, and particularly the prediction of the final deposit thickness h_d as a function of the process parameter and physico-chemical features of the ink, is still a major issue.

Many works previously reported in the literature have clearly identified two regimes for such flow-coating-like processes depending of the coating speed V [4-6]. At high V, a liquid film is drawn out of the reservoir and dries later on. In this regime, often referred to as the *Landau-Levich* regime, drying and coating are separated in time, and the height of the liquid film results from a balance between surface tension and friction induced by the substrate motion [7, 8]. At low V, solvent evaporation cannot be neglected during the film withdrawal, and the coating process yields directly a dry deposit: this is the evaporative regime.

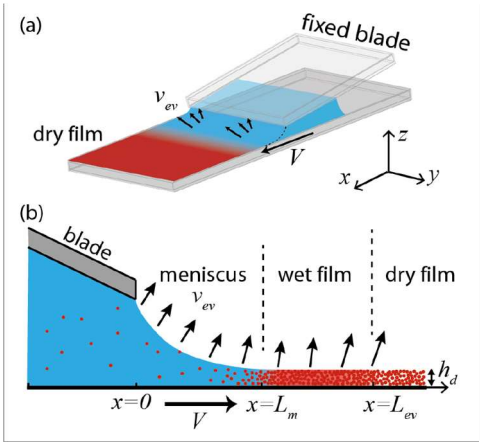

Figure 1: (a) Perspective view of a blade coating process in the evaporative regime. A dry film is continuously withdrawn from the reservoir by the substrate moving at a velocity V. (b) Side view evidencing the specific case of a colloidal dispersion. A solvent-saturated film is drawn out of a liquid reservoir and maintained by capillary forces between the blade and the moving substrate. Solidification occurs at a distance $x = L_m$, followed by a pore-emptying front at $x = L_{ev}$; arrows show schematically the local evaporative flux v_{ev} (m/s, see text).

In the last few years, many groups performed experimental and theoretical investigations of this evaporative regime for dilute inks ranging from colloidal dispersions [5,9-14] to solutions of polymers and small molecules [4,14-16]. Despite the wide complexity of the process and the wide variety of reported

phenomena, including streaks or stripes formation [17-19], cracks and delamination [20] to name a few, many of the above cited works reported the following scaling:

$$h_d \propto \frac{\varphi_0}{V} \quad (1)$$

for the dry deposit thickness h_d as a function of the substrate velocity V and the reservoir particle volume fraction φ_0. Such a robust scaling suggests a common explanation based on mass conservation arguments only. Assuming that coatings are uniform along their width (invariance to translation along the y-direction, see Figure 1), simple mass balances for a binary mixture (volatile solvent + non-volatile solute) provide the following relation for the deposit thickness [9]:

$$h_d = \frac{\varphi_0}{\varphi_c(1-\varphi_0)}\frac{Q_{ev}}{V} \quad (2)$$

where φ_0 and φ_c are the volume fractions of the non-volatile solute in the bulk meniscus and in the dry film, respectively, and Q_{ev} (m^2/s) is the solvent volume rate of evaporation per unit of width W. Eq. (2) points out the important role played by the solvent mass transfer in the vapor phase to get a quantitative prediction of Q_{ev} and thus h_d. One recovers the scaling reported experimentally and given by eq. (1) in the case of a dilute

ink $\varphi_0 << \varphi_c$ and assuming that Q_{ev} does not depend on φ_0, φ_c and V. This behavior was for instance observed in previous experiments performed in dip-coating-like configurations [4, 5, 14] Q_{ev} was shown to depend only on drying air characteristics (temperature, humidity, ...) and evaporation occurred over a constant length of the order of the meniscus size Lm [14]. Recently, several groups suggested that the case of colloidal dispersions is expected to be more intricate than the case of molecular solutes, and a significant departure from scaling (1) was even reported by Joshi and Gilchrist [21]. Indeed, the coating flow first leads to a wet film of densely-packed colloids, which ultimately dries later on at a distance $L_{ev} \geq L_m$ from the static blade, see Figure 1(b). This specific feature is related to the porous nature of the dry deposit, which can thus remain wet when capillary forces are strong enough to prevent the receding of the solvent through the pores of the coating, the so-called pore emptying [22, 23]. In the case of colloidal dispersions, the evaporation length L_{ev} now becomes a function of the process parameters, and can modify the solvent volume rate of evaporation Q_{ev}, as, in some cases, L_{ev} can be much larger than the meniscus length Lm. Jung and Ahn [24] along with Joshi and Gilchrist [21] have considered Darcy's law to model solvent transport in the wet porous film and have assumed the uniformity of evaporation intensity along the film, which results in the expression

$$Q_{ev} \simeq v_{ev} L_{ev} \quad (3)$$

They further derived the following scaling

$$h_d \propto \frac{\varphi_0^2 v_{ev}}{V^2} \quad (4)$$

for dilute dispersions $\varphi_0 << \varphi_c$, assuming a criterion for estimating the pore-emptying front from the liquid pore pressure. The latter scaling fits correctly the data sets reported by Joshi and Gilchrist [21]. However it fails to describe the experiments of refs [5, 11, 14] which support scaling (1) for colloidal dispersions, as well as measurements of the evaporation length L_{ev} reported by Jung and Ahn [24]. However, in the theories [21,24], evaporation is assumed to be dominated by the wet film only, i.e. $L_{ev} >> L_m$, and the contribution of the meniscus to the overall evaporation rate Q_{ev} is neglected.

In a recent study [25], we included this contribution, still assuming uniform evaporation as above, and we recovered scalings (1) and (4) as two asymptotic limits of the same model, the latter corresponding to $L_{ev} >> L_m$, the former to $L_{ev} \approx L_m$. We further showed that this continuous model agrees with the measure of L_{ev} performed by Jung and Ahn [24] as their experiments were performed in the transition regime between scalings (1) and (4).

It is important to underline that all these models are based on the assumption of a uniform evaporation velocity v_{ev} over the meniscus and the wet film. Indeed Eq. (3) implicitly contains the assumption of 1D vapor transfer in the gas phase. Real configurations, such as the experimental case described in Figure 1, are expected to yield multi-dimensional mass transfer (2D or even 3D), with spatial variations of v_{ev} all along the evaporation region. Indeed, the function Q_{ev} (L_{ev}) should depend on the mechanisms which drive the vapor transport in the gas phase: free or forced convection, laminar or turbulent flow, etc. For instance, Eq. (3) would be recovered for turbulent free convection, from which proportionality between Lev and Q_{ev} is expected, as derived by estimating mass transfer coefficients from empirical correlations (as available for instance in the book [26] using analogy between heat and mass transfer). In case of 3D vapor diffusion in quiescent air from a rectangular solvent puddle, a logarithmic dependence of Q_{ev} on the evaporation length is expected.

The main objective of the present work is to investigate the effect of multi-dimensional mass transfer in the gas phase on the evaporation length L_{ev} and the deposit thickness h_d, for blade-coating of colloidal dispersions in the evaporative regime. Using simplified models, we first provide analytical expressions of L_{ev} and h_d in asymptotic cases corresponding to 1D or 2D vapor transport.

These theoretical investigations help us to show that L_{ev} is strictly independent of the evaporation intensity, and nearly independent of the mass transfer nature, 1D or 2D. Conversely, the deposit thickness strongly depends on the of vapor motion in the gas phase, and different scaling laws are obtained for the 1D and 2D cases. We finally compare these theoretical predictions to experimental results obtained with a custom-made blade coating setup in a wide range of parameters (concentration, colloid particle diameters, coating speed) and to data previously reported in the literature. Experimental evaporation lengths L_{ev} are in very good agreement with our simplified theoretical model of mass transfer in the gas phase. This comparison also suggests that 3D effects may be relevant for quantitative predictions of the deposit thickness.

References

1. Sondergaard, R.; Hösel, M.; Angmo, D.; Larsen-Olsen, T.; Krebs, F. C., Mater. Today 2012, 15, 36-49.
2. Gu, X.; Yan, H.; Kurosawa, T.; Schroeder, B. C.; Gu, K. L.; Zhou, Y.; to, J. W. F.; Oosterhout, S. D.; Savikhin, V.; Molina-Lopez, F.; Tassone, C. J.; Mannsfeld, S. C. B.; Wang, C.; Toney, M. F.; Bao, Z., Adv. Energy Mater. 2016, 6, 1601225.
3. Prevo, B. G.; Kuncicky, D. M.; Velev, O. D., Colloids Surf., A 2007, 311, 2-10.
4. Le Berre, M.; Chen, Y.; Baigl, D, Langmuir 2009, 25, 2554-2557.
5. Grosso, D. J. Mater. Chem. 2011, 21, 17033-17038.
6. Berteloot, G.; Pham, C.-T.; Daerr, A.; Lequeux, F.; Limat, L.. Europhys. Lett. 2008, 83, 14003.
7. Weinstein, S.; Ruschak, K. Coating Flows. Annu. Rev. Fluid Mech. 2004, 36, 29-53.
8. Davis, R.; Jayaraman, S.; Chaikin, P.; Register, R. Langmuir 2014, 30, 5637-5644.
9. Dimitrov, A. S.; Nagayama, K. Continuous Langmuir 1996, 12, 1303-1311.
10. Berteloot, G.; Daerr, A.; Lequeux, F. Chem. Eng. Proc. 2013, 68, 69-73.
11. Prevo, B. G.; Velev, O. D. Langmuir 2004, 20, 2099.
12. Kuncicky, D.; Naik, R.; Velev, O. Small 2006, 2, 1462-1466.
13. Brewer, D. D.; Shibuta, T.; Francis, L.; Kumar, S.; Tsapatsis, M. Langmuir 2011, 27, 11660.
14. Jing, G.; Bodiguel, H.; Doumenc, F.; Sultan, E.; Guerrier, B. Langmuir 2010, 26, 2288-2293.
15. Maloy, S. F.; Martin, G. L.; Atanassov, P.; Cooney, M. J. Langmuir 2012, 28, 2589-2595.
16. Diao, Y.; Tee, B. C.-K.; Giri, G.; Xu, J.; Kim, D. H.; Becerril, H. A.; Stoltenberg, R. M.; Lee, T. H.; Xue, G.; Mannsfeld, S. C. B.; Bao, Z. Nat. Mater. 2013, 12, 665-671.
17. Bodiguel, H.; Doumenc, F.; Guerrier, B. Langmuir 2010, 26, 10758-10763.
18. Mino, Y.; Watanabe, S.; Miyahara, M. T. Langmuir 2015, 31, 41214128.
19. Boettcher, J. M.; Joy, M.; Joshi, K.; Muangnapoh, T.; Gilchrist, J. F.Langmuir 2015, 31, 10935.
20. Routh, A. F. Rep. Prog. Phys. 2013, 76, 046603.
21. Joshi, K.; Gilchrist, J. J. Colloid Interface Sci. 2017, 496, 222 - 227.
22. Routh, A. F.; Russel, W. B. AIChE J. 1998, 44, 2088-2098.
23. Goehring, L.; Clegg, W. J.; Routh, A. F.Langmuir 2010, 26, 9269-9275.
24. Jung, Y. D.; Ahn, K. H. Langmuir 2013, 29, 15762-15769.
25. Doumenc, F.; Salmon, J. B.; Guerrier, B. Langmuir 2016, 32, 13657-13668.
26. Rhosenow, W.; Hartnett, J.; Cho, Y. McGraw-Hill: New York, USA, 1998.